Heavy Ion Physics at the LHC*

R. Vogt[a,b]

[a]Lawrence Berkeley National Laboratory, Berkeley, CA USA

[b]Physics Department, University of California, Davis, CA USA

The ion-ion center of mass energies at the LHC will exceed that at RHIC by nearly a factor of 30, providing exciting opportunities for addressing unique physics issues in a completely new energy domain. Some highlights of this new physics domain are presented here. We briefly describe how these collisions will provide new insights into the high density, low momentum gluon content of the nucleus expected to dominate the dynamics of the early state of the system. We then discuss how the dense initial state of the nucleus affects the lifetime and temperature of the produced system. Finally, we explain how the high energy domain of the LHC allows abundant production of 'rare' processes, hard probes calculable in perturbative quantum chromodynamics, QCD. At the LHC, high momentum jets and $b\overline{b}$ bound states, the Υ family, will be produced with high statistics for the first time in heavy ion collisions.

1. QUANTIFYING THE INITIAL STATE

An accelerated nucleus may be envisioned as a lattice of valence quarks surrounded by sea quark and gluon fields. Although these sea quarks and gluons carry only a small fraction, x, of the total nucleon momentum, their density is very high, especially for the gluons. As the energy of the ion beam is increased, the lowest x values probed decreases while the density increases. Typical x values of partons produced at midrapidity, $y = 0$, with transverse momentum of $p_T \approx 2$ GeV/c at RHIC are $x \sim 2p_T/\sqrt{s_{NN}} \sim 0.02$ where the gluon density is not yet very high. However, the factor of 30 increase in energy between RHIC and the LHC decreases the x values correspondingly to $\sim 6.7 \times 10^{-4}$ where the gluon density is quite high. Expanding the rapidity coverage to the forward region further reduces the x values probed while increasing the gluon density still more.

At these high gluon densities where x is low and the 4-momentum transfer squared, Q^2, is moderate, the Q^2 evolution of the gluon densities can no longer be described by standard, linear evolution in Q^2. Instead, in the regime $1.5 \leq Q^2 \leq 10$ GeV^2 and $10^{-5} \leq x \leq 5 \times 10^{-3}$, nonlinear evolution of the parton densities dominates. The gluon wavelengths are long enough that they overlap each other and begin to interact, leading

*This work was supported in part by the Director, Office of Energy Research, Division of Nuclear Physics of the Office of High Energy and Nuclear Physics of the U. S. Department of Energy under Contract No. DE-AC03-76SF0098.

to terms with squared gluon densities at low x. At still smaller x, $x \leq 10^{-5}$, the gluon density is so large that it saturates the available phase space and the dynamics of the interaction may be described in terms of classical color fields.

Although the numbers given here are relevant for pp collisions where the gluons in a single nucleon begin to overlap each other, since the nonlinear growth of the gluon density depends on the transverse size of the system, these effects, as well as the subsequent saturation physics, may be expected to set in at higher x for nuclei than for free nucleons. Thus the initial state of the system and the gross properties of the system may be calculable in perturbative QCD.

The LHC energy domain is clearly in the regime where small x effects and departures from linear Q^2 evolution of the parton distributions will be prominent. Systematic studies of proton-proton, pp, and proton (or deuteron)-nucleus, $p(\mathrm{d})A$, collisions can yield much exciting information about the initial state of nucleus-nucleus, AA, collisions. The pp collisions will be at the highest energy, $\sqrt{s} = 14$ TeV, and therefore the lowest x. These collisions can study the nonlinear evolution regime and probe the onset of saturation in the proton. Studies of pPb or dPb collisions at 8.8 and 6.2 TeV/nucleon respectively, can elucidate the difference between the saturation regimes of the proton and the nucleus, providing the baseline nuclear parton distributions necessary to fully understand Pb+Pb collisions at $\sqrt{s_{NN}} = 5.5$ TeV/nucleon.

Another important characteristic of the initial state is its baryon number. One expects that, during the course of the collision, the valence quarks will be swept away from the center of the reaction zone, taking the total baryon number with them to the fragmentation regions. As a result, protons and antiprotons should be produced in equal abundance in the central region at sufficiently high energies. A manifestation of this is the measurement of the antiproton-to-proton ratio, $\overline{p}/p$, which has been shown to grow with energy. The most recent measurements at RHIC indicate $\overline{p}/p \sim 0.65$ in $\sqrt{s_{NN}} = 130$ GeV Au+Au collisions [1], growing to ~ 0.77 for $\sqrt{s_{NN}} = 200$ GeV [2,3]. The increase of this ratio with energy strongly suggests that, while a baryon free regime has not yet been reached at RHIC, the chances for reaching this regime at the LHC are quite good.

Thus the initial state of nuclear collisions at the LHC can be characterized by near zero baryon density and high initial gluon densities that may be described in terms of classical color fields. The initial state may be most cleanly studied in pA interactions where the multiplicities are still small. In addition, the best probes of such matter are those which do not interact strongly such as real and virtual photons and massive gauge bosons, the $W^{\pm}$ and Z^0.

We know from low energy deep-inelastic scattering that the nuclear parton distributions are modified relative to those of the free proton. However, the measurements are not very sensitive to the gluon distributions and the low x measurements are limited to rather small Q^2, $Q^2 \ll 1$ GeV^2. At the LHC however, the low x region can be effectively probed in the perturbative regime, up to $Q^2 \geq m_Z^2$. Massive gauge boson production proceeds predominantly through the $q\overline{q}$ channel rather than by gluons. Thus gauge boson production is an efficient probe of the high Q^2 quark and antiquark distributions. At RHIC, only the upper pp energy is large enough for statistically significant studies of $W^{\pm}$ and Z^0 production since the rates in the lower energy AA collisions are too small for meaningful measurements. High-statistics studies of the nuclear quark and antiquark densities at

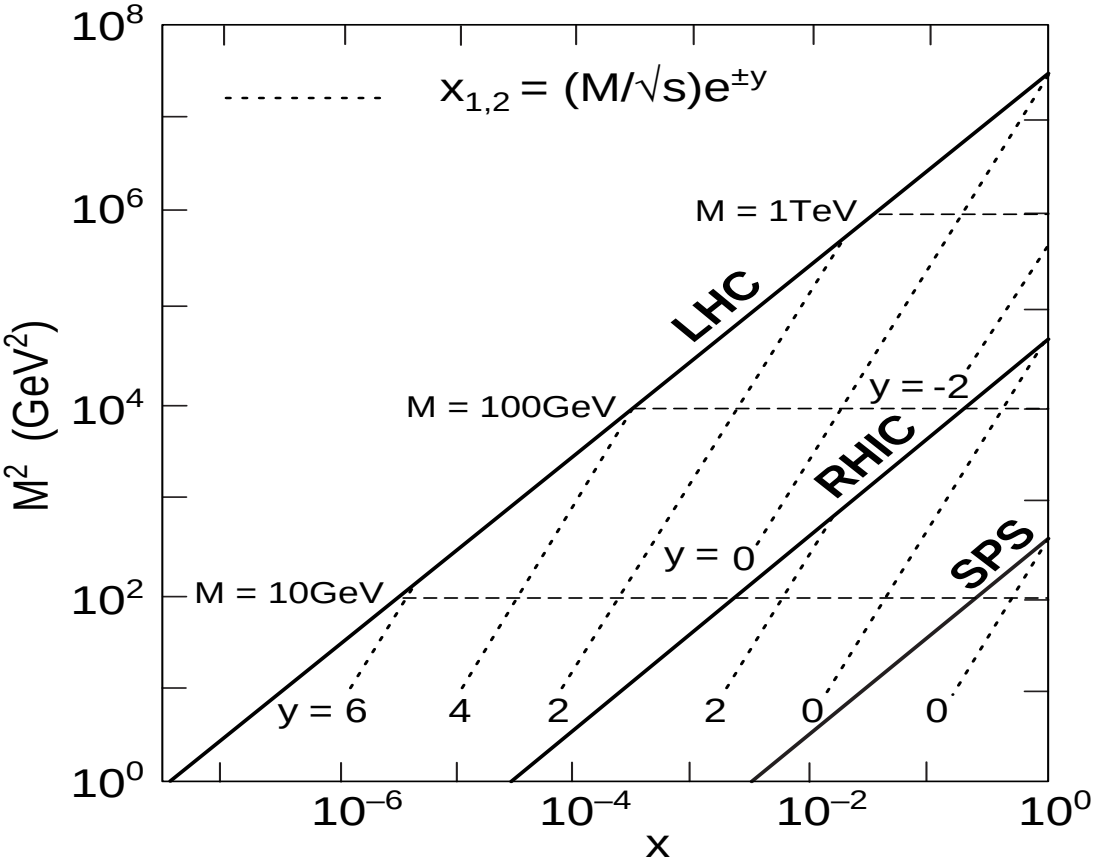

Figure 1. The $Q^2 = M^2 \geq 1$ GeV^2 reach as a function of x for the SPS, RHIC and the LHC. Lines of constant rapidity are indicated for each machine.

large momentum transfer, Q^2, through measurements of $W^{\pm}$ and Z^0 production would thus be unique to the LHC [4].

Direct photon production, on the other hand, is dominated by $qg \to q\gamma$ and can efficiently study the nuclear gluon distributions. Open charm production is another gluon-dominated process that helps determine the nuclear gluon distribution. We note that the effects of modified parton density evolution such as nonlinear and saturation effects should manifest themselves most strongly at low Q^2. Thus charm, with its relatively low mass, is also an important probe of the small x, low Q^2 regime [5]. Since modifications of the parton densities in nuclei have been observed when neither x nor Q^2 is small, measurements of the nuclear parton distributions at the LHC can help disentangle the different regimes of parton evolution.

2. THE FINAL STATE: HOTTER AND LONGER LIVED

Heavy ion collisions at LHC energies will explore regions of energy and particle density significantly beyond those reachable at RHIC. The energy density of the thermalized matter created at the LHC is estimated to be 20 times higher than at RHIC, implying

an initial temperature, T_0, nearly a factor of two higher than at RHIC [6]. The higher densities of the produced partons results in more rapid thermalization. Consequently, the time spent in the quark-gluon plasma phase, the difference between the plasma lifetime and the thermalization time, increases by almost a factor of three [6]. Thus the hot, dense systems created in heavy ion collisions at the LHC spend more time in a purely partonic state. The longer lifetime of the quark-gluon plasma state widens the time window available to probe it experimentally, as seen in Table 1.

Table 1
The initial QGP production time, lifetime, initial temperature and energy density for the maximum energy and mass systems at the SPS, RHIC and the LHC. From Ref. [6].

System	$\sqrt{s_{NN}}$ (GeV)	τ_0 (fm)	$\tau_{\rm tot}$ (fm)	T_0 (MeV)	ϵ_0 (GeV/fm^3)
SPS (Pb+Pb)	17	0.8	$1.4-2$	$210-240$	$1.5-2.5$
RHIC (Au+Au)	200	0.6	$6-7$	$380-400$	$14-20$
LHC (Pb+Pb)	5500	0.2	$18-23$	$710-850$	$190-400$

3. ABUNDANT HARD PROBES

Semi-hard and hard parton processes dominate particle production at the LHC. These hard probes [7], such as high-p_T jets and photons, quarkonia, and $W^{\pm}$ or Z^0 bosons, are characterized by the Q^2 necessary for their production. At the high collision energies of the LHC, the cross sections for processes with $Q^2 > (50\,{\rm GeV})^2$ are large enough for detailed systematic studies.

To better illustrate the large rates available for hard probes at the LHC, in Table 2 we present the minimum bias jet and gauge boson rates in the region $|\eta| \leq 2.4$ as well as the total $Q\overline{Q}$ and quarkonium rates calculated in perturbative QCD in Pb+Pb collisions at $\sqrt{s_{NN}} = 5.5$ TeV and pPb collisions at $\sqrt{s_{NN}} = 8.8$ TeV. The results are given for a 10^6 s LHC run in each case. We have assumed a luminosity of 5×10^{26} cm^{-2}s^{-1} for Pb+Pb [8] and a maximum pPb luminosity of 1.4×10^{30} cm^{-2}s^{-1} [9]. Conventional nuclear shadowing, the only nuclear effect included, is typically rather small for jets and gauge bosons but can be large for heavy quarks and quarkonium. The quarkonium rates include the branching ratios to lepton pairs.

4. MODIFICATION OF JETS IN DENSE MATTER

High p_T quark and gluon jets can be used to study the the hot medium produced after the collision. The large Q^2 of these jets causes them to materialize immediately after the collision. They are then embedded in and propagate through the dense environment as it forms and evolves. Through their interactions with the medium, they measure its properties and are thus sensitive to the formation of a quark-gluon plasma. Large transverse momentum probes are easily isolated experimentally from the soft particle background of

Table 2
The yield of hard probes in a 10^6 s LHC run.

	Pb+Pb $\sqrt{s_{NN}} = 5.5$ TeV $\mathcal{L} = 5 \times 10^{26}$ cm^{-2}s^{-1}		pPb $\sqrt{s_{NN}} = 8.8$ TeV $\mathcal{L} = 1.4 \times 10^{30}$ cm^{-2}s^{-1}	
Process	Yield/10^6 s	Ref.	Yield/10^6 s	Ref.
$\|\eta\| \leq 2.4$				
jet($p_T > 50$ GeV)	2.2×10^7	[10]	1.5×10^{10}	[9]
jet($p_T > 250$ GeV)	2.2×10^3	[10]	5.2×10^6	[9]
Z^0	3.2×10^5	[4]	6.8×10^6	[9]
W^+	5.0×10^5	[4]	1.1×10^7	[9]
W^-	5.3×10^5	[4]	1.1×10^7	[9]
all phase space				
$c\overline{c}$	9.0×10^{10}	[11]	2.0×10^{12}	[11]
$b\overline{b}$	3.6×10^9	[11]	8.2×10^{10}	[11]
$J/\psi \to \mu^+\mu^-$	2.4×10^7	[12]	5.5×10^8	[12]
$\Upsilon \to \mu^+\mu^-$	1.5×10^5	[12]	3.5×10^6	[12]
$\Upsilon' \to \mu^+\mu^-$	3.7×10^4	[12]	8.4×10^5	[12]
$\Upsilon'' \to \mu^+\mu^-$	2.2×10^4	[12]	5.2×10^5	[12]

the collision. Their high p_T ensures that the medium effects are perturbatively calculable, strengthening their usefulness as quantitative diagnostic tools. At the LHC, the production rates for jets pairs with $p_T > 50$ GeV for a single jet are several orders of magnitude larger than at RHIC. Indeed, more than 10 jet pairs are produced every second in Pb+Pb collisions at the LHC, as shown in the previous section. Thus high statistics systematic studies are possible in a clean kinematic regime, far beyond the limits of RHIC.

Jet pairs should be produced back to back. However, one or both of the jets can be modified by the medium. Interactions with the medium can reduce the jet energy and change its direction. In fact, some jets may lose so much of their initial energy that their energy is dissipated and they no longer appear as individual jets. The appearance of monojets was suggested as an early measure of 'jet quenching' due to energy loss [13]. At RHIC, evidence for such an effect has been measured through leading hadron correlations. In peripheral heavy ion collisions, two high p_T hadrons are detected back to back, similar to the measurements of pp interactions at the same energy. However, in central collisions, the opposite side hadron has disappeared and the azimuthal correlation is similar to that of the underlying soft hadrons in the event [14]. This jet suppression is absent in dAu collisions at RHIC, strongly suggesting that the suppression is a final-state effect arising from the dense medium. Such leading hadron measurements are also possible at the LHC. In addition, at the higher energy, the measurements can be performed for full jets rather than leading hadrons and extended to significantly higher p_T.

The dijet probe is nontrivial because the original energy of both jets is unknown. It would be preferable to have a method of tagging jets of known energy to measure the

energy loss [15]. Quark jets of known energy can be produced in reactions such as $gq \to q\gamma$ or $gq \to qZ^0$. In these cases, the energy is known since, to tree level, the quark jet is produced with transverse momentum equal and opposite to that of the gauge boson which is unaffected by the presence of the medium. While the reaction $gq \to qZ^0$ is a small contribution to the total Z^0 yield [4], it is a more distinctive signature since the Z^0 is free from the high background of hadronic decays contributing to the direct photon spectrum [16]. At the LHC, the Z^0+jet yield is large enough to extract physics signals. Any energy loss suffered by the jet can thus be more cleanly identified than in the dijet channel.

The measured energy loss yields the opacity of the medium: the product of the interaction cross section between the hard probe and the partonic medium with its density [17,18]. In kinematic regions where the rescattering cross section can be reliably calculated, the opacity provides access to the parton density after the collision, determining how the medium is affected by gluon saturation.

In addition to the dijet and jet+γ, Z^0 measurements, other measurements of high p_T jets and hadrons may also be important for quantifying the energy loss. We discuss three of these below: jet fragmentation, jet shapes and high p_T heavy quarks.

While the initial hard scattering can be described in terms of proton and nuclear parton distribution functions, the process by which the produced partons become the measured final state hadrons are characterized by fragmentation functions. These fragmentation functions are typically studied in e^+e^- collisions and then applied to other processes since they are assumed to be universal. However, because the parton distribution functions are known to be modified by the presence of the nuclear medium, one might also expect the fragmentation functions to be modified in the medium as well. The medium in question could either be cold matter, as studied in eA collisions at HERA [19], or hot and dense matter, produced in heavy ion collisions. Medium-modified fragmentation functions have been calculated by averaging the vacuum fragmentation function over the parton energy loss in the medium, weighted by the probability for the parton to lose energy. The jet suppression effects seen at RHIC are compatible with jet quenching [10]. Extrapolating from RHIC to the LHC based on the expected gluon multiplicity at each energy, one can expect similar suppression at $p_T > 50$ GeV in Pb+Pb collisions at the LHC.

One might also tend to expect that energy loss would modify the final shape of the produced jet. Recent calculations have found that such modifications are small. While energy loss does not strongly modify the jet shape, it can significantly change the multiplicity distribution inside the jet cone, increasing the multiplicity by more than a factor of two [10]. A measurement of the p_T distribution of produced hadrons relative to the jet axis may be very sensitive to the p_T broadening of the parton shower. Such measurements are only possible at the LHC where fully formed high p_T jets are observable.

Heavy quark production is copious at the LHC. These quarks tend to be produced in the early stages of the collision because their mass is typically much larger than the temperature of the medium. While in the medium, these quarks can also undergo energy loss. Recent calculations indicate that this loss may be rather small. However, the loss might be observable in either the dilepton or single lepton channels at large invariant mass or large p_T respectively, particularly for the b quarks [10].

5. Υ SUPPRESSION AS A QUARK-GLUON PLASMA PROBE

One of the proposed signatures of the QCD phase transition is the suppression of quarkonium production [20,21]. Suppression of the J/ψ and ψ' has been observed in nucleus-nucleus collisions at the CERN SPS [22]. In a plasma, the suppression occurs due to the shielding of the $c\overline{c}$ binding potential by color screening, leading to the breakup of the resonance. The $c\overline{c}$ and $b\overline{b}$ resonances have smaller radii than light-quark hadrons and therefore need higher temperatures to break up. Because the Υ is much smaller than the $c\overline{c}$ and other $b\overline{b}$ resonances, a much higher temperature is needed to dissociate the Υ [21]. Therefore it was previously assumed that the Υ would not be suppressed by QGP production [21,23].

In view of the high initial temperature of a gluon-dominated minijet plasma, $T \sim 0.9-1$ GeV [24], it was shown that, depending upon the properties of the plasma, the Υ could be suppressed, providing a valuable tool to determine the initial state of the system and the characteristics of the plasma [25]. With such high temperatures, strong plasma suppression might be expected. Unfortunately the short equilibration time of the minijet system correspondingly reduces the plasma lifetime in the scaling expansion, causing the minijet plasma to be too short-lived to produce quarkonium suppression in some cases. Alternatively, the initial conditions could be dominated by kinetic equilibration processes [26] with a correspondingly longer equilibration time, $t_0 \sim 0.5 - 0.7$ fm. Because the equilibration time of the parton gas is longer than that obtained from the minijet initial conditions, the time the system spends above the breakup temperature is also longer, leading to stronger suppression even though T_0 is lower.

Table 3
LHC values of t_D, and $p_{T\mathrm{m}}$, Ref. [16].

	$\mu \propto gT$, $n_f = 3$, $T_c = 170$ MeV		$\mu = 4T$, $T_c = 260$ MeV	
parton gas, $T_0 = 820$ MeV, $t_0 = 0.5$ fm				
	t_D (fm)	$p_{T\mathrm{m}}$ (GeV)	t_D (fm)	$p_{T\mathrm{m}}$ (GeV)
Υ	-	0	4.6	56.53
Υ'	4.79	23.16	15.69	81.98
χ_b	8.90	32.42	15.69	58.9
minijet plasma, no shadowing				
	$T_0 = 820$ MeV, $t_0 = 0.1$ fm		$T_0 = 1.05$ GeV, $t_0 = 0.1$ fm	
	t_D (fm)	$p_{T\mathrm{m}}$ (GeV)	t_D (fm)	$p_{T\mathrm{m}}$ (GeV)
Υ	-	0	1.94	22.2
Υ'	-	0	6.59	33.2
χ_b	-	0	6.59	23.05
minijet plasma, HPC shadowing[27]				
	$T_0 = 699$ MeV, $t_0 = 0.1$ fm		$T_0 = 897$ MeV, $t_0 = 0.1$ fm	
	t_D (fm)	$p_{T\mathrm{m}}$ (GeV)	t_D (fm)	$p_{T\mathrm{m}}$ (GeV)
Υ	-	0	1.21	11.7
Υ'	-	0	4.11	19.2
χ_b	-	0	4.11	12.1

The time at which the temperature drops below T_D and the state can no longer be suppressed, $t_D = t_0(T_0/T_D)^3$, and the maximum quarkonium p_T for which the resonance is suppressed, $p_{T,\mathrm{m}} = M\sqrt{(t_D/\tau_F)^2 - 1}$, are given in Table 3 for $\mu(T) \propto gT$ with $n_f = 3$ and $\mu(T) = 4T$, SU(3) plasma with $T_c = 260$ MeV using the parton gas and minijet initial conditions. Results for the minijet initial conditions are given for the GRV 94 LO parton densities both without shadowing and HPC shadowing [27], resulting in the lowest temperatures obtained with shadowing [16]. Note that the reduction of the initial temperature due to shadowing significantly reduces the p_T range of the suppression. However, this result can be distinguished from a case with no significant shadowing and a plasma with a smaller spatial extent [25].

A high statistics study of quarkonium production ratios such as ψ'/ψ and Υ'/Υ as a function of p_T may provide a conclusive test of plasma production at high energies. However, before the efficacity of the measurement as a test of QGP formation is proven, the relative importance of other effects must be established. Although shadowing is important, the effects should cancel in ratios of quarkonium states with very similar masses. Nuclear absorption should also cancel if the quarkonium state interacts with nucleons while still in a preresonance color octet state [28]. Although the resonances can interact with comoving secondaries, the p_T dependence of these comover interactions is already weak at CERN SPS energies [29] and expected to be weaker at the LHC [25].

Thus, if the ratios exhibit a significant p_T-dependence at large p_T in AB collisions, it will be virtually certain that a quark gluon plasma was formed. The precise behavior of the ψ'/ψ and Υ'/Υ ratios can then be used to strongly constrain the QGP model parameters. In particular, the ratios will be very different if only the Υ' or ψ' is suppressed relative to the case where all quarkonium states are suppressed.

The Υ rate includes feeddown to the Υ from Υ', Υ'' and two sets of χ_b states and feeddown to the Υ' from the Υ'' and $\chi_b(2P)$ states. Thus in the Υ'/Υ ratio, all sources of Υ' and Υ, each associated with a different suppression factor, must be considered [25]:

$$\frac{\Upsilon'}{\Upsilon}\Big|_{\mathrm{indirect}} \equiv \frac{\Upsilon' + \chi_b(2P)(\to \Upsilon') + \Upsilon''(\to \Upsilon')}{\Upsilon + \chi_b(1P, 2P)(\to \Upsilon) + \Upsilon'(\to \Upsilon) + \Upsilon''(\to \Upsilon)}\,. \tag{1}$$

In computing this 'indirect' Υ'/Υ ratio it is assumed that the suppression factor is the same for the $\chi_b(2P)$ and $\chi_b(1P)$ states and that identical suppression factors can be used for the Υ' and Υ''. The relative production and suppression rates in the color evaporation model, including the χ_b states, can be found in Ref. [25].

Figure 2 gives the indirect ratios. In a parton gas assuming $\mu = 4T$, all the Υ states can be suppressed for $p_T > 50$ GeV, producing the rather flat ratio in the solid curve. A measurement at the 20% level is thus needed to distinguish between the pp ratio and the QGP prediction. Substantial systematic errors in the ratio could make the detection of a deviation quite difficult due to the slow variation with p_T. With the slowly growing screening mass, $\mu \propto gT$, the direct Υ rate is not suppressed while the Υ' and χ_b states are suppressed. Under these conditions, the indirect ratio is less than the pp value until the Υ' is no longer suppressed and then is slightly enhanced by the χ_b decays until they also no longer suffer from plasma effects. Thus although the indirect ratio is less sensitive to the plasma, the Υ'/Υ ratios can significantly constrain plasma models, especially if the quarkonium states can be measured with sufficient accuracy up to high p_T.

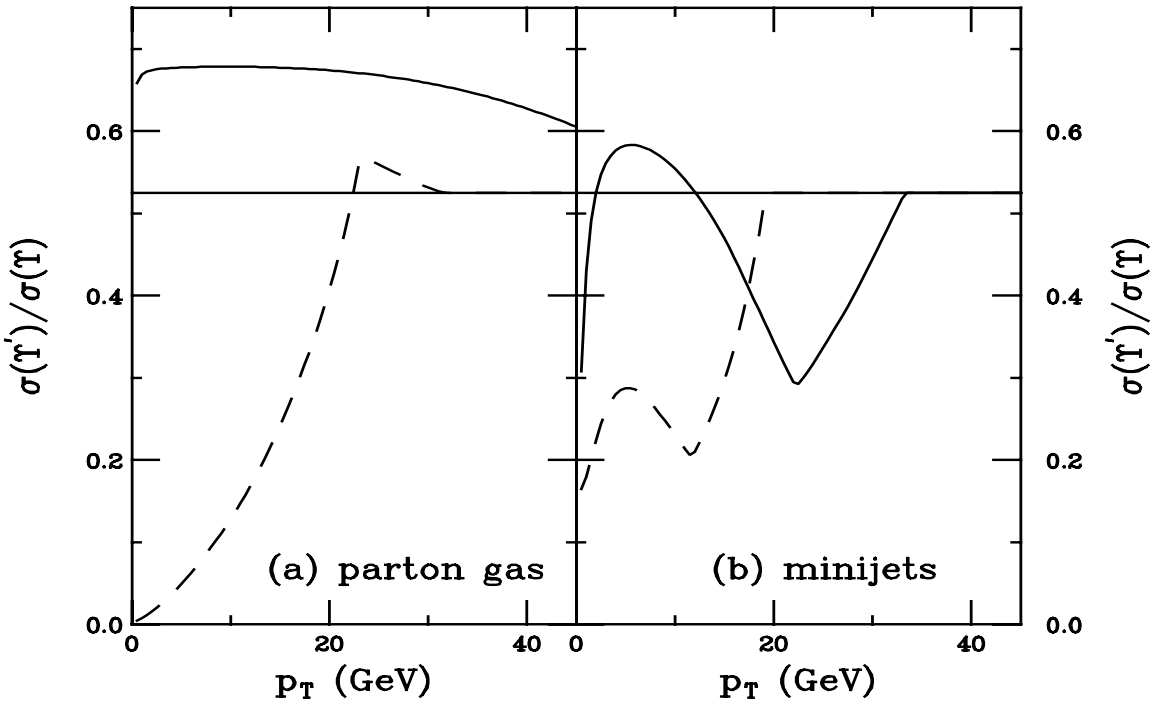

Figure 2. The Υ'/Υ ratio computed from Eq. (1) is shown for the initial conditions in Table 3 with $R = R_{\rm Pb}$. In (a), parton gas results are shown for $\mu \propto gT$ (dashed) and $\mu = 4T$ (solid). In (b) minijet results are given for $\mu = 4T$ without shadowing (solid) and with HPC shadowing (dashed). The horizontal curve represents the *pp* ratio. From [16].

6. SUMMARY

In this talk, we have presented only a few of the exciting new physics opportunities at the LHC. For more information on the dedicated heavy ion experiment ALICE, see the talk of C. Fabjan [30] and for a taste of the emerging ultra-peripheral heavy ion program at the LHC, see the talk of J. Nystrand [31]. The LHC will certainly turn lead-lead collisions into golden data.

REFERENCES

1. C. Adler *et al.* [STAR Collaboration], Phys. Rev. Lett. **86** (2001) 4778.
2. J.J. Gaardhøje *et al.* [BRAHMS Collaboration], arXiv:nucl-ex/0401026.
3. J. Adams, *et al.* [STAR Collaboration], arXiv:nucl-ex/0310004.
4. R. Vogt, Phys. Rev. C **64** (2001) 044901.
5. K.J. Eskola, V.J. Kolhinen and R. Vogt, Phys. Lett. B **582** (2004) 157.
6. I. Vitev, J. Phys. G**30** (2004) S791.
7. X.N. Wang, Phys. Rep. **280** (1997) 287.
8. D. Brandt, LHC Project Report 450, 2000.
9. A. Accardi *et al.*, arXiv:hep-ph/0308248.

10. A. Accardi *et al.*, arXiv:hep-ph/0310274.
11. R. Vogt, Int. J. Mod. Phys. E**12** (2003) 211.
12. M. Bedjidian *et al.*, arXiv:hep-ph/0311048.
13. M. Gyulassy and M. Plumer, Phys. Lett. B **243** (1990) 432.
14. C. Adler *et al.* [STAR Collaboration], Phys. Rev. Lett. **90** (2003) 082302.
15. X.N. Wang, Z. Huang, and I. Sarcevic, Phys. Rev. Lett. **77** (1996) 231.
16. G. Baur *et al.*, CMS/2000-60, 2000.
17. M. Gyulassy, P. Levai and I. Vitev, Phys. Rev. Lett. **85** (2000) 5535.
18. U.A. Wiedemann, Nucl. Phys. B **588** (2000) 303.
19. A. Airapetian *et al.* [HERMES Collaboration], Eur. Phys. J. C **20** (2001) 479.
20. T. Matsui and H. Satz, Phys. Lett. B **178** (1986) 416.
21. F. Karsch, M.T. Mehr, and H. Satz, Z. Phys. C **37** (1988) 617.
22. M.C. Abreu *et al.* [NA50 Collaboration], Phys. Lett. B **410** (1997) 327; 337.
23. F. Karsch and H. Satz, Z. Phys C **51** (1991) 209.
24. K.J. Eskola and K. Kajantie, Z. Phys. C **75** (1997) 515.
25. J.F. Gunion and R. Vogt, Nucl. Phys. B **492** (1997) 301.
26. X.M. Xu, D. Kharzeev, H. Satz and X.N. Wang, Phys. Rev. C **53** (1996) 3051.
27. K.J. Eskola, J. Qiu and J. Czyzewski, private communication.
28. D. Kharzeev and H. Satz, Phys. Lett. B **366** (1996) 316.
29. J. Ftaćnik, P. Lichard, J. Pišút, Phys. Lett. B **207** (1988) 194; S. Gavin, M. Gyulassy and A. Jackson, Phys. Lett. B **207** (1988) 257; R. Vogt, M. Prakash, P. Koch and T.H. Hansson, Phys. Lett. B **207** (1988) 263; J. Ftaćnik, P. Lichard, N. Pišútova and J. Pišút, Z. Phys. C **42** (1989) 132.
30. C. Fabjan, these proceedings.
31. J. Nystrand, these proceedings.